Inorg. Chem. **1993,** *32,* 3890–3894

Resonance Raman and Time-Resolved Resonance Raman Studies of Tris(4-methyl-2,2′-bipyridine)ruthenium(II). Polarization of the Radical Fragment of the ^{3}MLCT States

Shelly M. Treffert-Ziemelis, Janusz Golus, Dennis P. Strommen,[†] and James R. Kincaid[*]

Chemistry Department, Marquette University, Milwaukee, Wisconsin 53233

Received January 28, 1993

The resonance Raman (RR) and time-resolved resonance Raman (TR^3) spectra are reported for the tris(4-methyl-2,2′-bipyridine)ruthenium(II) complex, Ru(mmb)$_3^{2+}$, and its methyl-deuteriated analogue, Ru(d_3-mmb)$_3^{2+}$. The spectra are compared to those of tris(2,2′-bipyridine)ruthenium(II), Ru(bpy)$_3^{2+}$, and tris(4,4-dimethyl-2,2′-bipyridine)-ruthenium(II), Ru(dmb)$_3^{2+}$, and its methyl-deuteriated analogue Ru(d_6-dmb)$_3^{2+}$. The spectra of the ground state of the complex with the asymmetric ligand, mmb, are readily interpretable in terms of vibrationally isolated fragments (pyridine and 4-methylpyridine) with the exception of a few modes which are assignable to stretches of the inter-ring and adjacent bands. The TR^3 spectra are shown to be consistent with slight polarization of the ^{3}MLCT excited-state charge distribution toward the pyridine fragment of the chelated anion.

Introduction

As the interest and activity in the study of the long-lived ^{3}MLCT states of divalent ruthenium complexes of polypyridines and related ligands continues to intensify,[1] because of their inherent fundamental interest as well as their potential utility in solar energy conversion schemes, it becomes increasingly important to establish effective methods and strategies to probe the nature of these states. Following the pioneering work of Dallinger, Woodruff, and co-workers,[2] resonance Raman (RR) and time-resolved resonance Raman (TR^3) methods have been proven to be especially well suited for this purpose.[3]

Recently, for example, TR^3 methods were employed to definitively document selective localization of excited-state electron density on particular chelate rings in various heteroleptic complexes such as Ru(bpy)$_2$(bpz)$^{2+}$, where the proper formulation of the ^{3}MLCT state was shown to be $[Ru^{3+}(bpy)_2(bpz^{-})]^{2+}$.[3e] More recently, interest has developed in the study of complexes containing asymmetric chelates, such as 2-(2′-pyridyl)pyrimidine, which exhibit unique photophysical properties.[4] In view of this fact, RR and TR^3 studies of complexes of 2-(2′-pyridyl)pyrazine were completed which provided definite evidence for enhanced localization of the "radical-ligand" electron density on the pyrazine fragment of the chelate.[5]

In the present work this issue of enhanced localization effects is addressed for the case of a relatively mild modification of the bipyridine ligand, i.e., methylation of one of the pyridine fragments. The results document the spectroscopic consequences of such substituent-induced asymmetry and are intrepretable in terms of polarization of the ^{3}MLCT state electron density toward the pyridine fragment of the asymmetric chelate ring bearing the "optical electron".

Experimental Section

Preparation of Compounds. (A) Ligands. The ligand 4-methyl-2,2′-bipyridine (mmb) was prepared by following literature procedures.[6,7] Briefly, 1-(2-pyridinylcarbonyl)pyridinium iodide was prepared by treatment of a solution containing 2.42 g (0.02 mol) of freshly distilled 2-acetylpyridine (Aldrich) in 5 mL of dry pyridine (Aldrich) at 20 °C with 5.1 g (0.02 mol) of iodine in 15 mL of dry pyridine. This mixture was then heated to 100 °C and stirred for 3 h. After 3 h the heating bath was removed and the mixture was allowed to stand overnight. The crude crystals were filtered out and washed with pyridine. Recrystallization (2 times) from 18% ethanol/water in the presence of activated charcoal yielded 2.5 g (39%) of pure creamy glittery leaflets of 1-(2-pyridinylcarbonyl)pyridinium iodide (mp 197–198 °C lit. mp 198–199 °C).[7] The mmb ligand was prepared from 1-(2-pyridinylcarbonyl)pyridinium iodide by dissolving the salt in methanol under nitrogen and treating it with a stoichiometric amount of 2-butenal (crotonaldehyde) and an excess (approximately 10 equiv) of ammonium acetate. The solution was heated at 60–65 °C for 5 h, after which the methanol was removed under nitrogen. The residue was dissolved in 25 mL of water and extracted with ethyl ether (4 × 10 mL) followed by hexane (2 × 10 mL). The combined organic extracts were washed with water until the water layer was colorless. The organic solvent layer was then dried over sodium sulfate, filtered, and dehydrated under nitrogen. The product was then purified on a basic alumina column (22 × 1.5 cm) eluting with hexane/acetone (1/1). The compound was then further purified by sublimation: mp 63–64 °C (lit. mp 62–64 °C);[8] yield = 112 mg (10.7%).

The deuterated complexes, 4-C^{2}H$_3$-2,2′-bpy (d_3-mmb) and 4,4′-(C^{2}H$_3$)$_2$-2,2′-bpy (d_6-dmb), were prepared via the base-catalyzed H/D exchange of the methyl protons using the procedure of Godziela et al.[9] Briefly, 0.3 mmol of the methylated bipyridine was refluxed in 10 mL of DMSO-d_6 (Aldrich) under nitrogen. To this solution was added 1 equiv (per methyl group) of tetrabutyl ammonium hydroxide (2 M solution in methanol) (Aldrich), and the solution was refluxed for 6 h. The reaction

---

[†] Present address: Department of Chemistry, Idaho State University, Pocatello, ID 83209-8023.

(1) (a) Juris, A.; Balzani, V.; Barigelletti, F.; Campagna, S.; Belser, P.; Von Zelewesky, A. *Coord. Chem. Rev.* **1988,** *84,* 85. (b) Kalyanasundaram, K. *Coord. Chem. Rev.* **1982,** *46,* 159. (c) DeArmond, M. K.; Carlin, C. M. *Coord. Chem. Rev.* **1981,** *36,* 325. (d) Kalyanasundaram, K.; Grätzel, M.; Pelizetti, E. *Coord. Chem. Rev.* **1986,** *69,* 57. (e) Meyer, T. J. *Pure Appl. Chem.* **1986,** *58,* 1193.

(2) Bradley, P. G.; Kress, N.; Hornberger, B. A.; Dallinger, R. F.; Woodruff, W. H. *J. Am. Chem. Soc.* **1981,** *103,* 7441.

(3) (a) Smothers, W. K.; Wrighton, M. S. *J. Am. Chem. Soc.* **1983,** *105,* 1067. (b) McClanahan, S.; Hayes, T.; Kincaid, J. *J. Am. Chem. Soc.* **1983,** *103,* 4486. (c) Balk, R. W.; Stufkens, D. J.; Crutchley, R. J.; Lever, A. B. P. *Inorg. Chim. Acta* **1982,** *64,* L49. (d) Mabrouk, P. A.; Wrighton, M. S. *Inorg. Chem.* **1986,** *25,* 526. (e) Danzer, G. D.; Kincaid, J. R. *J. Phys. Chem.* **1990,** *94,* 3976. (f) Mallick, P. K.; Strommen, D. P.; Kincaid, J. R. *J. Am. Chem. Soc.* **1990,** *112,* 1686. (g) Chung, Y. C.; Leventis, N.; Wagner, P. J.; Leroi, G. E. *J. Am. Chem. Soc.* **1985,** *107,* 1416. (h) Orman, L. K.; Chang, Y. S.; Anderson, D. R.; Yube, T.; Xu, Xiaubing; Yu, Soo-Chang; Hopkins, J. B. *J. Chem. Phys.* **1989,** *90,* 1469. (i) Carrol, P. J.; Brus, L. E. *J. Am. Chem. Soc.* **1987,** *109,* 7613.

(4) Rillema, D. P.; Blanton, C. B.; Shaver, R. J.; Jackman, D. C.; Boldaji, M.; Bundy, S.; Worl, L. A.; Meyer, T. J. *Inorg. Chem.* **1992,** *31,* 1600.

(5) Danzer, G. D.; Golus, J. A.; Kincaid, J. R. *J. Am. Chem. Soc.*, in press.

(6) Huang, T. L. J.; Brewer, D. G. *Can. J. Chem.* **1981,** *59,* 1689.

(7) Krohnke, F.; Gross, K. F. *Chem. Ber.* **1959,** *92,* 22.

(8) Potts, K. T.; Winslow, P. A. *J. Org. Chem.* **1985,** *50,* 5405.

(9) Godziela, G. M.; Kramer, S. K.; Goff, H. M. *Inorg. Chem.* **1986,** *25,* 4286.

0020-1669/93/1332-3890$04.00/0

mixture was cooled in an ice bath, and 2 or 3 drops of 2 M aqueous HCL was added. The solution was mixed with 40 mL of water and immediately extracted with dichloromethane (3 × 20 mL). The combined organic phases (colorless) were washed with water and then dried over magnesium sulfate and filtered. Dichloromethane was removed under reduced pressure, and the resulting white residue was purified by sublimation. The extent of deuteriation was checked by NMR and GC/MS.

The samples of 2,2′-bipyridine (bpy) and 4,4′-dimethylbipyridine (dmb) were purchased from Aldrich Chemical Co. and sublimed prior to use.

(B) Preparation of the Complexes. The homoleptic complexes RuL_3^{2+}, L = bpy, 4-mmb, and dmb, and corresponding deuterated analogues were prepared by following literature procedures.[10-12] The heteroleptic complexes $RuL_nL'_{3-n}{}^{2+}$ were prepared using previously reported methods.[13-15]

(C) Spectral Measurements. Resonance Raman (RR) and time-resolved resonance Raman (TR^3) spectra were acquired as described previously.[16,17] The RR spectra were obtained from solutions which were (1–4) × 10^{-3} M in metal complex. The 1004-cm^{-1} band of toluene (Aldrich) was scanned prior to acquisition of the RR spectra to ensure correct positioning of the monochromator (±0.25 cm^{-1}). The monochromator was stepped using increments of 0.5 cm^{-1} unless otherwise noted.

The RR spectra were obtained using the excitation lines of a Spectra-Physics Model 2025-05 argon ion laser (457.9 nm) or a Coherent Model Innova-100-K3 krypton laser (356.4 nm). The TR^3 spectra were obtained as described previously[16,17] with the third harmonic (354.7 nm) of a Quanta-Ray (Spectra Physics) Model DCR-3A Nd: YAG laser (operated at 20 Hz). The TR^3 spectra were collected using monochromator steps of 1 cm^{-1} and an integration time of 2.5 s.

Results and Discussion

Ground-State Raman Spectra. The RR spectra (ground-state complexes) of the tris-homoleptic complexes with the three ligands of relevance here (i.e., bpy, dmb, and mmb), along with those of the corresponding deuteriated ligands of interest (d_6-dmb and d_3-mmb), are given in Figure 1. The spectrum of $Ru(bpy)_3^{2+}$ has been thoroughly investigated previously, and the spectral assignments have been supported by a reliable normal coordinate analysis (NCA), using data for 12 isotopomeric analogues.[16,17] Briefly, the spectrum is interpretable in terms of a 21 atom unit of C_{2v} symmetry which gives rise to 20 in-plane Raman-active (A_1) modes, the highest four of which are ν(C–H) stretches occurring above 3000 cm^{-1}. These high-frequency modes are well removed from the stretching and deformation modes associated with the aromatic core, which appear between ~1600 and 200 cm^{-1}. Thus, there are several C–C and C–N stretching coordinates which combine with four CCH (in-plane) bending coordinates to give rise to 11 modes between about 1600 and 1000 cm^{-1}. These are labeled as ν_5–ν_{15} in trace A of Figure 1. Two other key modes (ν_{16} and ν_{17}) involve mainly δ(CCC) and δ(CCN) bending motions mixed with δ(CCH) deformation and are observed between 600 and 800 cm^{-1}.

The spectrum of the $Ru(dmb)_3^{2+}$ complex can be interpreted similarly with the understanding that one of the totally symmetric ν(C–H) stretches is replaced by a $\nu(C_4–C_{Me})$ stretch which is expected to occur below 1000 cm^{-1} but may mix with ring stretching and deformation modes. This would lead to one additional mode being active in the frequency region between ~1600 and 200 cm^{-1}. In order to clarify the discussion, the symbols ω_l have been adopted for labeling the modes of the dmb complexes and the highest frequency "core mode" occurring near 1600 cm^{-1} has been designated as ω_5 merely for the purpose of making convenient comparisons with the corresponding modes of the bpy complexes (i.e., one of the ν(C–H) stretches is replaced by $\nu(C_4–C_{Me})$ and ω_5 is actually the fourth highest frequency mode).

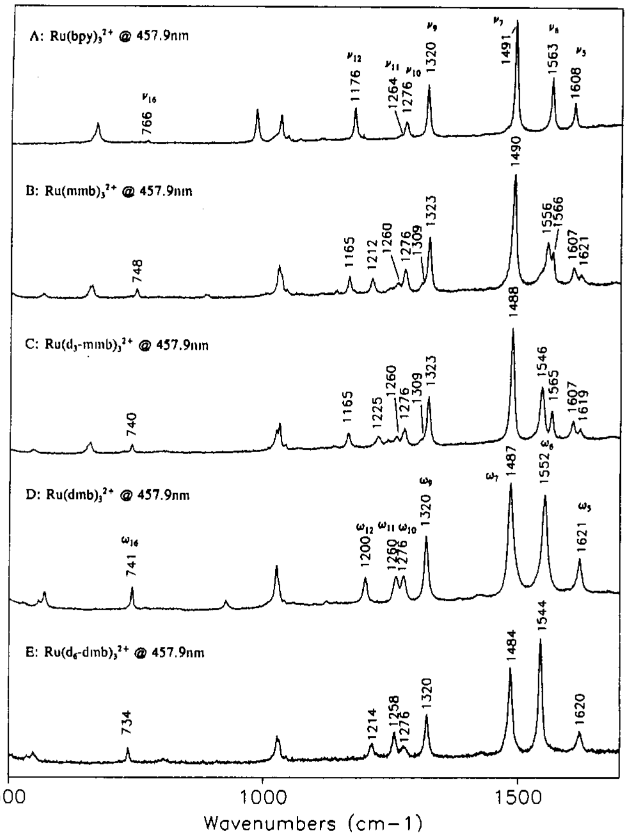

Figure 1. Ground-state resonance Raman spectra.

Finally, we note that the modes expected in the region below 1200 cm^{-1}, especially in the TR^3 spectra (vide infra), are often quite weak or unobservable. These modes were eventually located and identified in the case of $Ru(bpy)_3^{2+}$ (by intensive study of many isotopically labeled analogues).[16,17] While similar studies of the methylated complexes may have added an element of "completeness" to this study, no attempt was made to do this for the dmb (or mmb) complexes inasmuch as this is not necessary in order to establish the essential points of the present work. Thus, only the modes between ~1600 and 1200 cm^{-1} are labeled in Figures 1 and 2 and tabulated in Table I. The only exception to this statement is the inclusion of ν_{16} (ω_{16}) and ν_{16}' (ω_{16}'), which are readily observable, isolated modes occurring between 700 and 800 cm^{-1} in all of the complexes studied. Given this labeling scheme and interpretational strategy, attention is focused on the spectra of $Ru(mmb)_3^{2+}$ (trace B) and its deuteriated analogue, $Ru(d_3\text{-mmb})_3^{2+}$ (trace C). Upon comparison of the spectrum of $Ru(mmb)_3^{2+}$ (trace B) with those shown in traces A and D, it is immediately apparent that the RR spectrum of the complex bearing the asymmetric ligand can be viewed as a composite of the spectra of the corresponding complexes possessing symmetric ligands. Thus, many of the features observed in traces A and D appear at virtually identical positions in trace B, implying that, in general, the separate fragments of the asymmetric chelate are vibrationally isolated. Thus, ν_5 appears at 1608 cm^{-1} in trace B as well as in trace A, and ω_5 appears at 1621 cm^{-1} in traces B

---

(10) Evans, I. P.; Spencer, A.; Wilkinson, G. *J. Chem. Soc., Dalton Trans.* **1973**, 204.

(11) Crutchley, R. J.; Lever, A. B. P.; Lever, A. B. P. *J. Am. Chem. Soc.* **1980**, *102*, 7128.

(12) Crutchley, R. J.; Lever, A. B. P. *Inorg. Chem.* **1982**, *21*, 2276.

(13) McClanahan, S. F.; Dallinger, R. F.; Holler, F. J.; Kincaid, J. R. *J. Am. Chem. Soc.* **1985**, *107*, 4853.

(14) Sprintschinck, G.; Sprinschnick, H. W.; Kirsch, P. P.; Whitten, D. G. *J. Am. Chem. Soc.* **1977**, *99*, 4947.

(15) Crutchley, R. J.; Lever, A. B. P.; Poggi, A. *Inorg. Chem.* **1983**, *22*, 2647.

(16) Mallick, P. K.; Danzer, G. D.; Strommen, D. P.; Kincaid, J. R. *J. Phys. Chem.* **1988**, *92*, 5628.

(17) Strommen, D. P.; Mallick, P. K.; Danzer, G. D.; Lumpkin, R. S.; Kincaid, J. R. *J. Phys. Chem.* **1990**, *94*, 1357.

(18) (a) Fuson, N.; Garrigou-Lagrange, C.; Josien, M. L. *Spectrochim. Acta* **1960**, *16*, 106. (b) Wilmshurst, J. K.; Bernstein, H. J. *Can. J. Chem.* **1957**, *35*, 911.

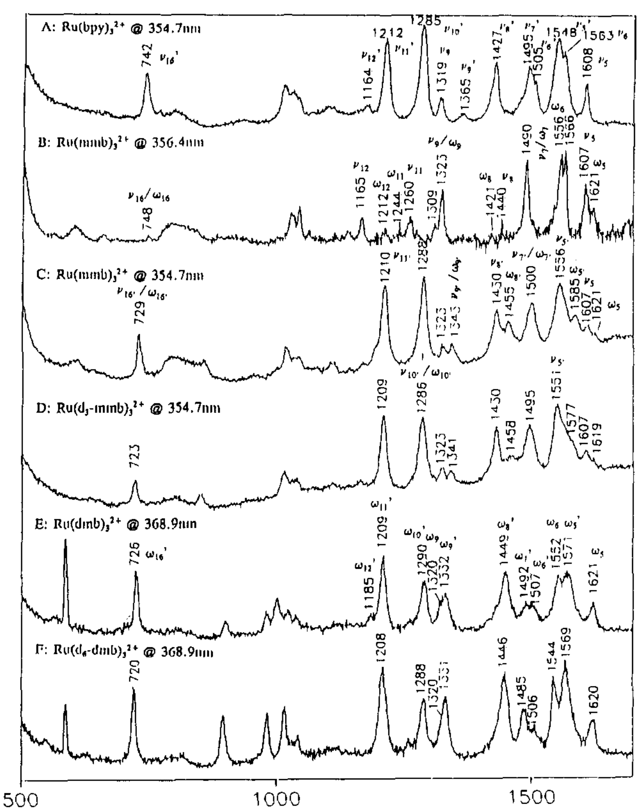

Figure 2. Time-resolved resonance Raman (TR^3) spectra.

and D. Similar behavior is observed for several other modes (e.g., ν_6 and ω_6 as well as ν_8 and ω_8).

Finally, it seems appropriate to mention that several modes which are apparently associated with a given fragment of the mmb ligand exhibit slightly different frequencies compared to the corresponding modes of the symmetric ligand. This behavior is observed for ν_8 (1450 cm^{-1} in bpy vs 1440 cm^{-1} in mmb), ν_{12} (1176 vs 1165 cm^{-1}), ω_{11} (1260 vs 1244 cm^{-1}), and ω_{12} (1200 vs 1212 cm^{-1}).

With reference to Table I, a comparison of the deuteration-induced shifts for $Ru(mmb)_3^{2+}/Ru(d_3\text{-}mmb)_3^{2+}$ vs $Ru(dmb)_3^{2+}/Ru(d_6\text{-}dmb)_3^{2+}$ confirms the preservation of the essential nature of the pyridine and methylpyridine modes and supports the general picture of vibrationally isolated peripheral segments of the asymmetric chelate. Thus, the "pyridine-like" modes associated with the peripheral bonds of the pyridine fragment (ν_5, ν_6, and ν_8) are observed at frequencies which are quite similar to their values in the case of $Ru(bpy)_3^{2+}$ and, as expected, exhibit insignificant shifts upon deuteriation of the methyl group. The modes associated with the periphery of the methylated ring (ω_5, ω_6, and ω_8) exhibit frequencies and deuteriation-induced shifts which agree well with those observed for the $Ru(dmb)_3^{2+}/Ru(d_6\text{-}dmb)_3^{2+}$ pair.

While the peripheral segments of each six-membered ring give rise to relatively isolated modes, the bonds associated with the central region of the chelate (i.e., the C_2–C_2', C_2–C_3, and C_2–N bonds) give rise to modes which appear at frequencies that are approximately intermediate between those corresponding to the complexes with the symmetric ligands. Thus, on the basis of a previous normal mode calculation[17] for $Ru(bpy)_3^{2+}$, it is expected that ν_7/ω_7, ν_9/ω_9, ν_{10}/ω_{10}, and ν_{16}/ω_{16} are the specific modes which contain large contributions from these particular bonds. As can be seen by inspection of Figure 1 and Table I, it is precisely these modes (labeled ν_7/ω_7, ν_9/ω_9, ν_{10}/ω_{10}, and ν_{16}/ω_{16}) for $Ru(mmb)_3^{2+}$ which exhibit this behavior. In the first three cases it is difficult to distinguish between the possibilities that one mode occurs at an intermediate frequency or that two modes are nearly accidently degenerate (although there is no evidence for broadening of these modes). The ν_{16}/ω_{16} mode clearly conforms to expected behavior inasmuch as a single band is observed at 748 cm^{-1} in the case of $Ru(mmb)_3^{2+}$ whereas the corresponding modes for $Ru(dmb)_3^{2+}$ and $Ru(bpy)_3^{2+}$ occur at 741 and 766 cm^{-1}, respectively.

In summary of this section, the RR spectrum of the ground state of $Ru(mmb)_3^{2+}$ is interpretable in terms of relatively isolated modes associated with the peripheral segments of each six-membered ring fragment of the chelate, as evidenced by frequencies and deuterium shifts which are quite similar to those for the symmetric complexes. On the other hand, several modes are associated with the central bonds region of the chelate and appear at frequencies which are intermediate between those observed for the two symmetric complexes.

Excited-State Raman Spectra. The TR^3 spectra of $Ru(mmb)_3^{2+}$ and its deuterated analogue, $Ru(d_3\text{-}mmb)_3^{2+}$, are given in Figure 2 along with those of the relevant reference complexes, $Ru(bpy)_3^{2+}$, $Ru(dmb)_3^{2+}$, and $Ru(d_6\text{-}dmb)_3^{2+}$. The spectrum of the ground-state complex, $Ru(mmb)_3^{2+}$, observed with 356-nm excitation, is also given (trace B) in order to support the assignment of certain features in the TR^3 spectrum to modes associated with coordinated neutral mmb ligands (vide infra).

Before proceeding to a detailed analysis of the spectrum of $Ru(mmb)_3^{2+}$, it is helpful to summarize the interpretation of the spectra of the two reference complexes, $Ru(bpy)_3^{2+}$ and $Ru(dmb)_3^{2+}$. The TR^3 spectrum of $Ru(bpy)_3^{2+}$ has been thoroughly studied and the interpretation supported by a detailed NCA which employed an extensive data set obtained for 12 isotopomers.[17] The spectrum is comprised of two sets of bands, one of whose frequencies and relative intensities are insignificantly different from those of $Ru(bpy)_3^{2+}$ and a second set whose frequencies and intensities are quite similar to the chemically-generated Libpy anion radical.[19] The TR^3 spectrum thus provides direct evidence for proper formulation of the ^{3}MLCT excited state as $[Ru^{3+}(bpy)_2(bpy^-)]^{2+}$. The features associated with the (bpy$^-$) are labeled ν_i' in trace A of Figure 2 (and in Table I), while those corresponding to the remaining two neutral ligands are labeled ν_i. We wish to point out that the relative intensities of the ν_i bands in trace A of Figure 2 are similar to those observed with 356-nm excitation (i.e., at approximately the same excitation wavelength (355 nm) used for the TR^3 measurements) and are not expected to be similar to those shown in Figure 1A, although, of course, the frequencies are identical.

The TR^3 spectrum of the other reference complex, $Ru(dmb)_3^{2+}$, has not been thoroughly studied as yet, but the data obtained here for the deuteriated analogue help to establish an interpretation similar to that given above for $Ru(bpy)_3^{2+}$. Careful inspection of the spectra given in traces E and F of Figure 2 lead to the correlation of ground to ^{3}MLCT state shifts which are given in Table I. The assignments given for both complexes of symmetric ligands indicate consistent behavior upon formation of the ^{3}MLCT states. Thus, there is a general lowering of frequencies as a result of population of the antibonding LUMO, though several modes (in each case) shift to higher frequencies. These shifts to higher frequencies have been shown to be the result of an increased bond strength of the C_2–C_2' bond in the ^{3}MLCT state, whereas the large downshits are attributed to weakening of the ring modes.[3f,17] As can be seen by inspection of Table I, ν_5, ν_6, and ν_{11} (as well as ω_5, ω_6, and ω_{11}) experience large downshifts, but the modes containing contributions from C_2–C_2' (ν_7–ν_{10} and ω_7–ω_{10}) exhibit smaller downshifts or shifts to higher frequency.

The TR^3 spectrum of $Ru(mmb)_3^{2+}$ shown in trace C of Figure 2 is quite complex, and proper identification of radical modes requires careful analysis and additional spectral measurements with ~370-nm excitation (Figure 3). In trace C of Figure 2 the

---

[19] Danzer, G. D.; Golus, J. A.; Strommen, D. P.; Kincaid, J. R. *J. Raman Spectrosc.* **1990**, *21*, 3.

Table I. Observed Ground-State and ^{3}MLCT Excited-State Frequencies

mode	$Ru(bpy)_3^{2+}$, $Ru(dmb)_3^{2+}$ (Δd)[a]	$Ru(bpy)_3^{2+\bullet}$, $Ru(dmb)_3^{2+\bullet}$ (Δd)[a]	$\Delta\nu/\nu'$,[b] $\Delta\omega/\omega'$ [b]	$Ru(mmb)_3^{2+}$ (Δd)[a]	$Ru(mmb)_3^{2+\bullet}$ (Δd)[a]	$\Delta\nu/\nu'$,[b] $\Delta\omega/\omega'$ [b]
ν_5/ν_5'	1608	1548	–60	1607 (0)	1554 (1)	–53
ω_5/ω_5'	1621 (1)	1571 (2)	–50	1621 (2)	1585 (4)	–36
ν_6/ν_6'	1563	1506	–57	1566 (1)	1508 (0)	–58
ω_6/ω_6'	1552 (8)	1507 (1)	–45	1556 (10)	1508 (0)	–46
ν_7/ν_7'	1491	1495	+4	1490 (2)	1500 (5)	+10
ω_7/ω_7'	1487 (3)	1492 (7)	+5			
ν_8/ν_8'	1450	1427	–23	1440 (0)	1430 (0)	–10
ω_8/ω_8'	1426 (0)	1449 (3)	+23	1421 (0)	1455 (+3)	+34
ν_9/ν_9'	1320	1365	+45	1323 (0)	1343 (2)	+20
ω_9/ω_9'	1320 (0)	1332 (1)	+12	[1309 (0)]		
ν_{10}/ν_{10}'	1276	1285	+9	1276 (0)	1286 (0)	+10
ω_{10}/ω_{10}'	1276 (0)	1290 (2)	+14			
ν_{11}/ν_{11}'	1264	1212	–52	1260 (0)	1210 (1)	–50
ω_{11}/ω_{11}'	1260 (2)	1209 (1)	–51	1244 (0)	N.O.[d]	
ν_{12}/ν_{12}'	1176	1164	–12	1165 (0)	N.O.[d]	
ω_{12}/ω_{12}'	1200 (+14)[c]	1185 (N.O.)[d]	–15	1212 (+13)	N.O.[d]	
ν_{16}/ν_{16}'	766	742	–24	748 (8)	729 (6)	–19
ω_{16}/ω_{16}'	741 (7)	726 (6)	–15			

[a] Frequency shifts caused by deuteration of the methyl group(s). [b] The difference in frequencies of the ground-state modes and the radical (excited-state) modes. [c] We note that similar behavior has been observed in the case of toluene where a ring mode at 1208 cm^{-1} shifts to 1226 cm^{-1} (i.e., +14 cm^{-1}) upon deuteration of the methyl groups.[18a] [d] N.O. indicates not observed.

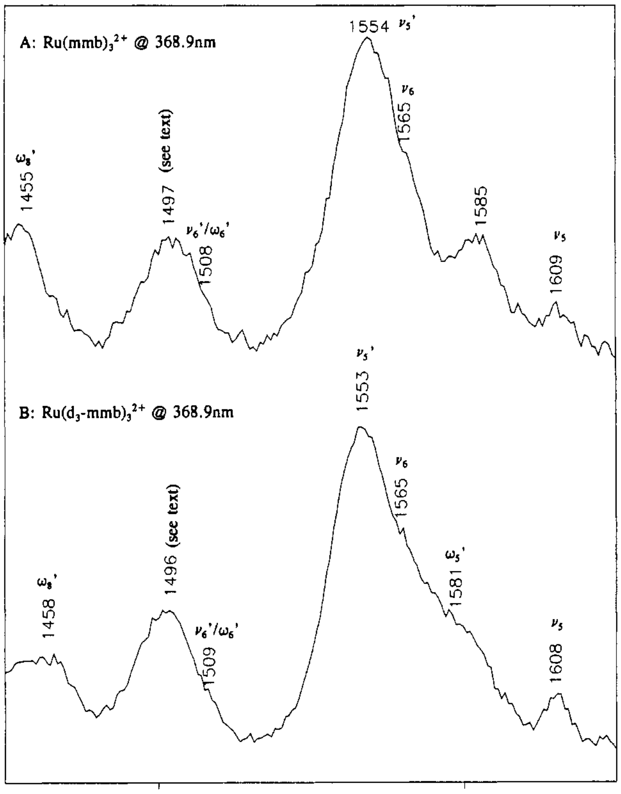

Figure 3. Time-resolved resonance Raman (TR^3) spectra.

features associated with the two coordinated "neutral" ligands (labeled ν_i, ω_i, and ν_i/ω_i) are, in general, identifiable by comparison with the spectrum given in trace B (i.e., the ground-state species obtained with 356-nm excitation). The modes associated with the radical fragment (mmb$^-$) in trace C (i.e., these labeled ν_i', ω_i', and ν_i'/ω_i') correspond reasonably well with the corresponding radical modes observed for $[Ru(bpy)_3^{2+}]^*$ (trace A) or $[Ru(dmb)_3^{2+}]^*$ (trace E), with a few important exceptions.

The most important difference is the appearance of a feature located at 1585 cm^{-1} in trace C, which is labeled as ω_5'. The spectra shown in Figure 3 yield a deuterium shift of 4 cm^{-1} for this mode, and it is thus correlated with the methylpyridine fragment. The next highest frequency radical mode occurs at ~1554 cm^{-1} and is labeled ν_5' (i.e., associated with the periphery of the pyridine fragment.) While an apparent (unexpected) deuterium shift is indicated by comparison of traces C and D in Figure 2, this is the result of the coincidence of this mode with the "neutral ligand" mode which occurs at 1556 cm^{-1} (which experiences a 10-cm^{-1} downshift upon deuteration). The greater enhancement of the radical component of the spectrum with 370-nm excitation (Figure 3) documents the lack of a deuterium shift in this mode.

The 1500-cm^{-1} region of the spectrum is especially complicated by the potential overlap of several different modes. Thus, a neutral ligand mode (ν_7/ω_7) may appear near this frequency (1490 cm^{-1}) and should exhibit only a 2-cm^{-1} deuterium shift. In addition, three radical modes are expected, ν_6' and ω_6' (near 1505 cm^{-1}) as well as ν_7'/ω_7' (near 1495 cm^{-1}), the latter of which may be expected to shift upon deuteration as was the case for ω_7' of $[Ru(dmb)_3^{2+}]^*$ (i.e., 1492 cm^{-1}, Δd = 7 cm^{-1}). The observed downshift of 5 cm^{-1} (1500–1495 cm^{-1}) observed upon comparison of traces C and D of Figure 2 must result from the presence of a deuterium-sensitive radical mode near this frequency inasmuch as the neutral ligand component would not exhibit such a shift (i.e., ν_7/ω_7 shifts by only 2 cm^{-1}). Identification of the other radical modes for $[Ru(mmb)_3^{2+}]$ is relatively straightforward and requires no discussion.

Structural Interpretation of the TR^3 Data. It is instructive to compare the ground-state to excited-state shifts ($\Delta\nu_i/\nu_i'$ and $\Delta\omega_i/\omega_i'$) listed in Table I for the three complexes studied. While, in general, the observed shifts agree well throughout the series, the key modes associated with the periphery of each six-membered ring fragment (i.e., ν_5/ν_5' and ω_5/ω_5') exhibit interesting behavior. Thus, in the case of the two symmetric complexes, $Ru(bpy)_3^{2+}$ and $Ru(dmb)_3^{2+}$, the shifts are ~60 cm^{-1} (ν_5/ν_5') and ~50 cm^{-1} (ω_5/ω_5'). Given a symmetric charge distribution on the coordinated (mmb$^-$) radical, one would expect approximately similar downshifts for ν_5/ν_5' and ω_5/ω_5'. As can be seen in Table I however, ω_5' shifts by only 36 cm^{-1} from its value for ω_5, a shift which implies a slightly stronger peripheral bond (i.e,. decreased excited-state charge density) for $Ru(mmb)_3^{2+}$ relative to $Ru(dmb)_3^{2+}$.

Such an implied asymmetric charge distribution is not completely unexpected inasmuch as the pyridine fragment is better able to stabilize the ^{3}MLCT state electron density. This statement is supported also by TR^3 data for a series of heteroleptic complexes with bipyridine and 4,4-dimethylbipyridine (i.e., $Ru(bpy)_n$-

$(dmb)_{3-n})$, where it was shown that there is a strong preference for population of the bpy ligand in the two heteroleptic complexes.[3d,13] Recent TR^3 studies of complexes of 2-(2′-pyridyl)pyrazine (pypz) also support this interpretation.[5] In that case, TR^3 evidence documents selective localization of (pypz$^-$) electron density on the pyrazine fragment, a result which is again consistent with TR^3 studies[3c] of the corresponding heteroleptic complexes $Ru(bpy)_2(bpz)^{2+}$ and $Ru(bpy)(bpz)_2{}^{2+}$.

Acknowledgment. This work was supported by a grant from the Department of Energy, Office of Basic Energy Sciences (Grant ER13619). Such support does not constitute an endorsement by DOE of the views expressed in this work. We also thank Dr. Gerald Danzer and Dr. Krzysztof Maruszewski for assistance in several Raman measurements. S.M.T.-Z. thanks the Department of Education for a National Needs Fellowship which partially supported this research.